OPEN

Postdeployment Respiratory Syndrome in Soldiers With Chronic Exertional Dyspnea

Sergey S. Gutor, MD, PhD, Bradley W. Richmond, MD, PhD,*† Rui-Hong Du, MD,* Pingsheng Wu, PhD,*‡ Kim L. Sandler, MD,§ Grant MacKinnon, MD,‖ Evan L. Brittain, MD,‖ Jae Woo Lee, MD,¶ Lorraine B. Ware, MD,*# James E. Loyd, MD,* Joyce E. Johnson, MD,# Robert F. Miller, MD,* John H. Newman, MD,* Stephen I. Rennard, MD,** Timothy S. Blackwell, MD,*† and Vasiliy V. Polosukhin, MD, PhD**

Abstract: After deployment to Southwest Asia, some soldiers develop persistent respiratory symptoms, including exercise intolerance and exertional dyspnea. We identified 50 soldiers with a history of deployment to Southwest Asia who presented with unexplained dyspnea and underwent an unrevealing clinical evaluation followed by surgical lung biopsy. Lung tissue specimens from 17 age-matched, nonsmoking subjects were used as controls. Quantitative histomorphometry was performed for evaluation of inflammation and pathologic remodeling of small airways, pulmonary vasculature, alveolar tissue and visceral pleura. Compared with control subjects, lung biopsies from affected soldiers revealed a variety of pathologic changes involving their distal lungs, particularly related to bronchovascular bundles. Bronchioles from soldiers had increased thickness of the lamina propria, smooth muscle hypertrophy, and increased collagen content. In adjacent arteries, smooth muscle hypertrophy and adventitial thickening resulted in increased wall-to-lumen ratio in affected soldiers. Infiltration of CD4 and CD8 T lymphocytes was noted within airway walls, along with increased formation of lymphoid follicles. In alveolar parenchyma, collagen and elastin content were increased and capillary density was reduced in interalveolar septa from soldiers compared to control subjects. In addition, pleural involvement with inflammation and/or fibrosis was present in the majority (92%) of soldiers. Clinical follow-up of 29 soldiers (ranging from 1 to 15 y) showed persistence of exertional dyspnea in all individuals and a decline in total lung capacity. Susceptible soldiers develop a postdeployment respiratory syndrome that includes exertional dyspnea and complex pathologic changes affecting small airways, pulmonary vasculature, alveolar tissue, and visceral pleura.

Key Words: US soldiers, deployment, exertional dyspnea, constrictive bronchiolitis

(*Am J Surg Pathol* 2021;45:1587–1596)

Since 2001, >2.7 million US military Service Members have been deployed in support of operations in Southwest Asia, including Iraq and Afghanistan.[1,2] An increased

From the *Department of Medicine, Division of Allergy, Pulmonary and Critical Care Medicine; Departments of §Radiology; #Pathology, Microbiology and Immunology, Vanderbilt University Medical Center; †Veterans Affairs Medical Center; ‡Department of Biostatistics, Vanderbilt University School of Medicine; ‖Department of Medicine, Division of Cardiovascular Medicine, Vanderbilt University Medical Center, Nashville, TN; ¶Department of Anesthesia and Perioperative Care, University of California, San Francisco, CA; and **Department of Medicine, Division of Pulmonary, Critical Care, Sleep and Allergy, University of Nebraska Medical Center, Omaha, NE.

Conflicts of Interest and Source of Funding: Supported by the Department of Defense W81XWH-17-1-0503, National Institutes of Health HL126176, generous donation by Ms. Carol Odess. S.I.R. was an employee of AstraZeneca from 2015 to 2019 and continues to own shares that were received as part of his compensation. As part of that employment, he represented AstraZeneca on the Board of Directors of Dizal Pharma without additional compensation. In the last 3 years, he has consulted for Bergenbio, GlaxoSmithKline, NovoVentures and Verona. Between 1996 and 2007, his university received funding from tobacco companies that supported studies relating to harm reduction and to the impact of tobacco smoke on stem cells. As part of this work, he consulted with RJ Reynolds without personal fee on the topic of harm reduction, received funding from RJ Reynolds to evaluate the effect of a harm reduction product in normal smokers (1996) and in subjects with chronic bronchitis (1999) and to assess the effect of smoking cessation on lower respiratory tract inflammation (2000); he participated in a Philip Morris multi-center study to assess biomarkers of smoke exposure (2002); he received funding for a clinical trial from the Institute for Science and Health (2005), which receives support from the tobacco industry, to evaluate biomarkers in exhaled breath associated with smoking cessation and reduction. This study was supplemented with funding from Lorillard and RJ Reynolds to expand the spectrum of biomarkers assessed. He received a grant from the Philip Morris External Research Program (2005) to assess the impact of cigarette smoking on circulating stem cells in the mouse. There are no active tobacco-industry funded projects. All ties with tobacco industry companies and entities supported by tobacco companies were terminated in 2007. For the remaining authors none were declared.

Correspondence: Vasiliy V. Polosukhin, MD, PhD, Department of Medicine, Division of Allergy, Pulmonary and Critical Care Medicine, Vanderbilt University Medical Center, T-1218 MCN, Nashville, TN 37232-2650 (e-mail: vasiliy.v.polosukhin@vumc.org).

Supplemental Digital Content is available for this article. Direct URL citations appear in the printed text and are provided in the HTML and PDF versions of this article on the journal's website, www.ajsp.com.

frequency of respiratory symptoms (such as persistent or recurrent cough, shortness of breath, and reduced exercise tolerance) has been documented in military personnel deployed to the region compared with nondeployed personnel.[3–5] While clinical evaluation of 380 deployed Military Service members with respiratory symptoms postdeployment revealed evidence of a variety of definable pulmonary conditions, including asthma, or laryngeal disorders, a large percentage (32.1%) of study participants had unexplained exertional dyspnea.[6]

In this regard, King et al[7] evaluated 49 US soldiers referred for unexplained postdeployment exertional dyspnea and exercise limitation. Thirty-eight of these soldiers were diagnosed with constrictive bronchiolitis based on findings from lung biopsies, despite the lack of fixed obstruction on pulmonary function testing (PFTs). While this report was supported by several other case reports,[8–10] concerns have been raised in the scientific community whether the reduced exercise tolerance could be explained by the reported pathology in small airways.[1,6,11–13] Therefore, to shed light on the nature of postdeployment dyspnea and exercise limitation, we undertook this study to perform a comprehensive, in-depth histopathologic evaluation of lung biopsy samples collected from US military Service Members after returning from deployment to Southwest Asia.

MATERIALS AND METHODS

Study Design

Lung biopsies were obtained by video-assisted thoracoscopic surgery from 50 soldiers with unexplained exertional dyspnea and exercise intolerance that appeared after deployment in Iraq and/or Afghanistan. Surgical lung biopsies were performed at Vanderbilt University Medical Center from 2004 to 2018 after ruling out identifiable cardiopulmonary disease by noninvasive testing. For this study, we selected all lung biopsies from individuals included in the prior report by King et al[7] that met criteria for morphometric evaluation (28 subjects). These criteria included the availability of at least 2 paraffin tissue blocks with 3 or more small airways in cross-section, along with minimal hemorrhagic and artifactual damage. We also obtained additional biopsies performed after the previous report that met the criteria described above (22 subjects). Each of these individuals had lung biopsy findings reported to be consistent with a diagnosis of constrictive bronchiolitis without evidence of other distinct lung pathologies, including granulomatous diseases, interstitial lung disease, or chronic obstructive pulmonary disease. For nondiseased (ND) control subjects, we obtained lung tissue samples from 17 age-matched lifelong nonsmokers without a history of chronic lung disease collected at the University of California San Francisco Medical Center. These lungs were rejected for lung transplantation and were donated for research purposes.

A clinical pathologic evaluation of each tissue sample was performed by an experienced clinical lung pathologist (J.E.J.), followed by quantitative histologic evaluation (histomorphometry) of lung specimens by study investigators (S.S.G. and V.V.P.) as described below. All available clinical data (deployment exposure, spirometry, high-resolution computed tomography [HRCT], and echocardiography) were analyzed and then correlated with histopathologic findings. The study protocol was approved by the Institutional Review Board at Vanderbilt University Medical Center (Nashville, TN) and University of California San Francisco Medical Center (San Francisco, CA).

Clinical Evaluation

All soldiers were evaluated with PFTs and scanning HRCT. PFTs included spirometry, lung volumes, and diffusing capacity for carbon monoxide (DLCO) performed according to American Thoracic Society guidelines.[14]

Computed tomography (CT) images were obtained with protocols in accordance with American College of Radiology standards to minimize radiation exposure to patients. High-resolution protocols routinely included prone and expiratory phase imaging. Images were interpreted at the time of acquisition and were also evaluated by a board-certified, cardiothoracic radiologist (K.L.S.) in accordance with study metrics to assess for variables including air trapping, basilar scarring, pulmonary fibrosis, nodularity, ground glass opacities and evidence of emphysema.

Echocardiographic data for this study were analyzed retrospectively from 25 soldiers using clinically indicated echocardiograms. All studies were performed on a Philips iE33 machine (the Netherlands) according to American Society of Echocardiography guidelines.[15,16] Data was analyzed by a board certified echocardiographer using AGFA software (Belgium).

Histopathologic Analysis and Morphometry

Four serial paraffin sections (5 μm) from each tissue block were used for hematoxylin and eosin, periodic acid-Schiff, Verhoeff-Van Gieson or PicroSirius red stains. Additional serial sections were used for immunostaining to detect immune inflammatory cells (CD4 or CD8 T cells, CD19 B cells or neutrophils), structural cells (smooth muscle or endothelial cells), and elastin. The list of antibodies and immunohistochemistry protocols are available in the online Supplement (Supplemental Digital Content 1, http://links.lww.com/PAS/B170).

Small airways < 2 mm in diameter were selected for examination. Larger airways containing mural cartilage or submucosal glands and airways > 2 mm in internal diameter were excluded from the analysis. Smaller respiratory bronchioles with discontinuous walls that opened into alveolar ducts were also excluded from examination. Each selected small airway was assessed for: (1) epithelial height ($V:SA_{EPI}$), (2) lamina propria thickness ($V:SA_{LP}$), (3) smooth muscle thickness ($V:SA_{SM}$), (4) adventitia thickness ($V:SA_{ADV}$), (5) collagen and elastin content, and (6) immune inflammatory cell (CD4 and CD8 lymphocytes and neutrophils) infiltrations according to ATS/ERS standards for Quantitative Assessment of Lung Structure in non-inflated lung biopsies.[17] Distal pulmonary arteries (blood vessels within bronchovascular bundles) were assessed for media ($V:SA_{MED}$) and adventitia ($V:SA_{ADV}$) thickness on

Verhoeff-Van Gieson stained sections. Wall-to-lumen ratio was calculated as a ratio of wall thickness (a sum of media and adventitia thicknesses) to luminal diameter (diameter of the circle formed by the full length of the basement membrane [BM]). Alveolar tissue was analyzed for blood capillary density, collagen content (LD_{COL}), and elastin content (LD_{ELAST}). The presence of lymphoid follicles was assessed on sections immunostained for CD19-expressing B cells. The visceral pleura was assessed on hematoxylin and eosin, periodic acid-Schiff, and PicroSirius red stained serial tissue sections. Further details of morphometric procedures are provided in Online Supplement (Supplemental Digital Content 1, http://links.lww.com/PAS/B170). The numbers of small airways and arteries examined per study participant and their BM lengths (airway/artery size) were similar across both study groups (Supplemental Table 1, Supplemental Digital Content 2, http://links.lww.com/PAS/B171). Morphometry was performed blinded to study group using Image-Pro Plus 7.0 (Media Cybernetics, Silver Springs, MD) or ImageJ 1.8.0 (NIH, Bethesda, MD) software.

Statistical Analysis

Demographic, clinical, morphologic, and physiologic data are reported as median (range) or mean ± SD according to their distributions. For categorical variables, proportions were used. Comparisons between symptomatic soldiers and ND controls were conducted using *t* test or Mann-Whitney *U* test for continuous variables and the χ^2 test for categorical variables. Follow-up data was compared with initial values by paired *t* test or paired Wilcoxon test according to distribution. Hierarchical cluster analysis was used to identify and differentiate subgroups based on pathologic patterns.[18] A hierarchical cluster tree (dendrogram) was constructed based on Euclidean distance. Subgroups were formed in an agglomerative manner, starting with each participant as his/her own subgroup and pairing the 2 closest subgroups together at every step until only 1 group of all participants remained. We applied the Average silhouette and Gap statistic method for determination of the optimal number of clusters.[19] The number of subgroups was also confirmed by a visual inspection of the dendrogram and a Multi-Dimensional Scaling plot. We applied the L1 penalty of the least absolute selection and shrinkage logistic regression to all morphometrical parameters to determine the features that distinguished affected soldiers from ND controls.[20] The optimal regularization parameters were chosen by 5-fold cross validation. All analyses were performed using R-software version 3.5.2 (www.r-project.org).

RESULTS

Study Participants Characteristics and Clinical Evaluation

As shown in Table 1, soldiers with exertional dyspnea and exercise intolerance were predominantly young (mean age 36 y), male, nonsmokers. During deployment, soldiers served in a variety of capacities, including helicopter pilots, flight engineers, infantry members, communication specialists, fuelers, mechanics, and military police. All affected soldiers reported exposure to environmental hazards during deployment. Of note, 23 soldiers served in northern Iraq in 2003 and reported exposure to smoke from a sulfur-mine fire near Mosul.[21] Soldiers also reported inhalation exposures to burn pits, dust storms, diesel exhaust, human waste and/or combat smoke (Table 2).

TABLE 1. Demographic Characteristics of Study Participants

Characteristics	ND Controls (N = 17)	Soldiers With Exertional Dyspnea (N = 50)
Age (y)	37 (20-50)	36 (26-55)
Sex (%)		
Male	12 (71)	47 (94)
Female	5 (29)	3 (6)
Smoking history (%)		
Lifelong nonsmokers	17 (100)	33 (66)
Current smokers	—	3 (6)
Former smokers	—	14 (28)

Median and range (minimum and maximum) are indicated for age. Number (percent) is indicated for sex and smoking history.

On PFTs, 17 soldiers had a reduction in carbon monoxide diffusing capacity (DLCO < 80% predicted), 2 had evidence of mild obstruction (forced expiratory volume in 1 second/forced vital capacity < 0.7) and 4 had mild restriction (total lung capacity [TLC] <80% predicted) (Table 2). Abnormalities were identified on chest HRCT from 23 soldiers, most commonly mild-to-moderate air trapping on expiratory scans (Table 2). All echocardiograms showed normal left and right ventricular function.

Clinical follow-up data were available on 29 of 50 soldiers (58%) with median follow-up period of 5 years (ranging from 1 to 15 y). All 29 soldiers reported continued

TABLE 2. Clinical Characteristics of Soldiers With Exertional Dyspnea

Characteristics	Value, N (%)
Reported exposures	
Sulfur dioxide	23 (46)
Burn pits	21 (42)
Dust storms	8 (16)
Burning oil, exhaust	3 (6)
Other (chemicals, industrial or combat smoke)	8 (16)
PFT	
Normal	30 (60)
Low DLCO (< 80% predicted)	17 (34)
Obstructive (FEV_1 < 80% predicted, FEV_1/FVC < 0.7)	2 (4)
Restrictive (TLC < 80% predicted)	4 (8)
HRCT	
Normal	27 (54)
Mild/moderate air trapping	19 (36)
Basilar scarring	2 (4)
Mild interstitial fibrosis	1 (2)
Micronodules	1 (2)
Peripheral and ground-glass infiltrate	2 (4)
Emphysema	1 (2)

FEV_1 indicates forced expiratory volume in 1 second; FVC, forced vital capacity.

TABLE 3. Longitudinal PFT Data (N = 29)

	PFTs (% Predicted)		
Parameters	**Original**	**Follow-up**	***P***
FEV_1	86.2 ± 13.6	86.3 ± 17.0	0.634
FVC	90.1 ± 13.8	86.4 ± 16.7	0.090
FEV_1/FVC	0.79 ± 0.05	0.80 ± 0.03	0.503
DLCO	85.8 ± 16.4	84.3 ± 16.4	0.548
TLC	98.4 ± 14.9	90.2 ± 14.9	< 0.001

Data presented as mean ± SD for PFT parameters (all normalized for age, sex, and height).

FEV_1 indicates forced expiratory volume in 1 second; FVC, forced vital capacity.

dyspnea on exertion, frequently accompanied by persistent cough and/or chest tightness. One soldier died from progressive interstitial lung disease not identified on initial evaluation. Among these 29 soldiers, TLC (% predicted) was reduced at the time of follow-up PFTs compared with disease presentation (Table 3) and 13/29 soldiers (44.8%) had a reduction in TLC of > 10% predicted on follow-up PFTs; however, the majority of these individuals had TLC values that remained within the normal range at follow-up (> 80% predicted). Seven soldiers (24.1%) had a reduction of forced vital capacity > 15% predicted on follow-up PFTs. Detailed information about follow-up clinical and PFT evaluation is available in Supplemental Table 2 (Supplemental Digital Content 3, http://links.lww.com/PAS/B172).

Pathologic Evaluation

Review of lung biopsies by an expert clinical lung pathologist confirmed the presence of small airway pathology in all 50 symptomatic soldiers (Fig. 1). All cases showed fibrous remodeling of bronchiolar walls consistent with constrictive bronchiolitis and in 12 cases macrophage infiltration within the bronchiolar lumen and peribronchiolar alveoli suggested a component of respiratory bronchiolitis (Supplemental Fig. 1, Supplemental Digital Content 4, http://links.lww.com/PAS/B173). To quantify pathologic changes in the lungs of these soldiers, we undertook a comprehensive morphometric evaluation of all distal lung compartments.

The most striking pathologic changes were observed in bronchovascular bundles, affecting both small airways and adjacent arteries. Bronchioles from affected soldiers showed increased thickness of the lamina propria, hypertrophy of smooth muscle, and increased collagen density

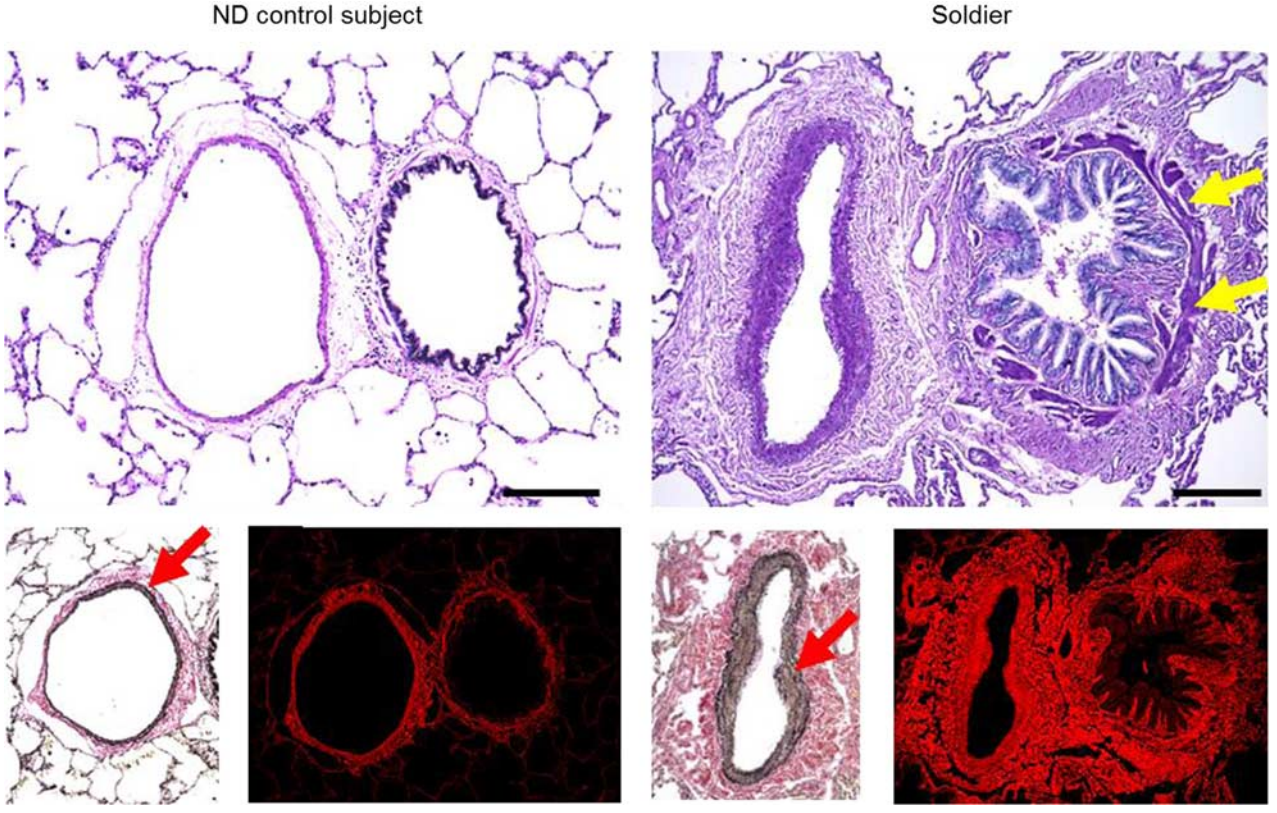

FIGURE 1. Histopathology of bronchovascular bundles. A—normal-appearing small airway and artery from ND control subject; small airway from soldier with moderate smooth muscle hypertrophy (yellow arrows), increased collagen density in subepithelium and constrictive-like luminal narrowing; pulmonary artery from soldier with increased medial thickness due to hypertrophy/hyperplasia of smooth muscle (red arrows). Top row: periodic acid-Schiff staining, bottom row—left images demonstrate moderate smooth muscle hypertrophy in pulmonary artery in soldier (Verhoeff-Van Gieson staining); right images demonstrate increased collagen density in small airway and arterial walls in soldier (collagen red fluorescence, PicroSirius red staining). Scale bars = 100 μm.

TABLE 4. Morphometric Evaluation of Lung Tissue Samples

Parameters	ND Controls (N = 17)	Soldiers With Exertional Dyspnea (N = 50)	*P*
Inflammatory cells in airway wall (n/mm)			
CD4 cells	9.5 (6.2, 12.1)	30.4 (24.8, 38.6)	< 0.001
CD8 cells	5.9 (3.5, 6.8)	17.9 (12.9, 26.8)	< 0.001
Neutrophils	4.6 (3.1, 5.7)	2.5 (1.0, 4.8)	< 0.05
Lymphoid follicles			
Adjacent to airways	2 (12%)	32 (64%)	< 0.001
In alveolar tissue (ie, beneath pleura)	1 (6%)	28 (56%)	< 0.001
Both	0	22 (44%)	< 0.001
Small airway walls			
Epithelial height ($V:SA_{EPI}$) (μm)	13.2 ± 1.1	13.1 ± 1.8	0.70
Lamina propria thickness ($V:SA_{LP}$) (μm)	12.4 ± 2.5	14.3 ± 2.8	< 0.05
Smooth muscle thickness ($V:SA_{SM}$) (μm)	6.1 ± 1.8	8.0 ± 1.9	< 0.001
Adventitia thickness ($V:SA_{ADV}$) (μm)	29.7 ± 5.7	30.3 ± 5.6	0.69
Collagen content (% of subepithelium)	26.6 (20.4, 28.6)	36.4 (29.5, 45.8)	< 0.001
Elastin content (% of subepithelium)	3.9 (2.6, 5.1)	4.0 (2.8, 6.4)	0.57
Arteries			
Smooth muscle thickness ($V:SA_{SM}$) (μm)	19.9 (15.2, 20.7)	38.4 (31.7, 50.7)	< 0.001
Adventitia thickness ($V:SA_{ADV}$) (μm)	37.5 (33.7, 39.6)	47.9 (40.5, 59.3)	< 0.001
Wall to internal diameter ratio	0.27 (0.22, 0.37)	0.44 (0.34, 0.61)	< 0.001
Alveolar tissue (interalveolar septa)			
Collagen content (LD_{COL}) (μm)	1.1 (0.1, 1.4)	2.0 (1.6, 2.3)	< 0.001
Elastin content (LD_{ELAST}) (μm)	0.7 (0.4, 0.8)	0.9 (0.8, 1.0)	< 0.001
Blood capillary density (LD_{CAP}) (n/mm)	69.4 ± 3.9	61.1 ± 5.2	< 0.001
Pleura			
Thickening	0	23 (46%)	< 0.001
Inflammatory cell infiltration	0	37 (74%)	< 0.001
Fibrosis	0	44 (88%)	< 0.001

Normally distributed numerical parameters are indicated as mean ± SD; non-normally distributed numerical parameters are indicated as median (interquartile range).

in the subepithelium (Fig. 1, Table 4). No differences were observed in epithelial height, adventitial thickness, or elastin content within the subepithelium.

In addition to remodeling of bronchiolar walls, evaluation of immune/inflammatory cells revealed > 3-fold increase in CD4 and CD8 T cells within the airway walls (Table 4). In contrast, no increase in neutrophils was observed in affected soldiers compared with ND controls. In addition to lymphocytic inflammation within the airway walls, we observed B cell-containing lymphoid follicles in close proximity to small airways in 64% of soldiers and within alveolar tissue in 56% of soldiers (Supplemental Fig. 2, Supplemental Digital Content 5, http://links.lww.com/PAS/B174; Table 4). For comparison, lymphoid follicles were rarely present in ND control lungs (12% had lymphoid follicles adjacent to small airways and 6% within alveolar tissue). Furthermore, diffuse infiltration of CD4 and CD8 T cells was observed in lung parenchyma and pleura from affected soldiers (Supplemental Figs. 3, 4, Supplemental Digital Contents 6 and 7, http://links.lww.com/PAS/B175, http://links.lww.com/PAS/B176).

In distal pulmonary arteries adjacent to bronchioles, medial thickness (due to smooth muscle hyperplasia/hypertrophy) was significantly increased in lungs of affected soldiers (Fig. 1, Table 4). Increased adventitial thickness due to edema and fibrosis was also identified in these arteries (Table 4). The combination of pathologic changes in the media and adventitia of arteries resulted in a marked increase in the wall-to-lumen ratio of these blood vessels (Table 4). In addition to pathologic changes in arteries adjacent to small airways, we observed remodeling of distal vasculature within the lung parenchyma. Abnormal muscularization, excessive collagen deposition, and increased wall thickness were present in distal pulmonary arteries adjacent to respiratory bronchioles (Fig. 2A).

In the alveolar compartment, we observed increased wall thickness of distal venules with collagen deposition in the adventitia (Figs. 2B, C). Evaluation of the interalveolar septa (IAS) revealed a reduction in blood capillary density in lungs of affected soldiers (Fig. 2D, Table 4). In addition, the IAS in affected soldiers showed a diffuse fibrotic phenotype with increased deposits of collagen and elastin, but without distortion of alveolar architecture (Fig. 3A, Table 4).

Pathologic changes of visceral pleura, which were not observed in ND controls, were present in 92% of affected soldiers (Fig. 3B, Table 4). Pleural pathology was characterized by: (1) infiltration of mononuclear inflammatory cells (mostly lymphocytes) within and beneath the pleural lining (54% of affected soldiers), (2) pleural thickening (46% of affected soldiers), and/or (3) increased collagen deposition (fibrosis) identified on PicroSirius red staining (88% of affected soldiers). Together, histomorphometric evaluation of lungs from affected soldiers showed diffuse and distinctive pathology in all distal lung compartments.

Hierarchical Clustering Analysis

To investigate whether pathologic findings in the lungs could effectively separate diseased soldiers from ND controls, we performed unsupervised hierarchical clustering based on morphometric parameters. This analysis showed complete separation of these 2 groups (Fig. 4A). Further analysis showed that the optimal number of clusters was 2, indicating a relatively homogenous disease group (Fig. 4B; Supplemental Fig. 5, Supplemental Digital Content 8, http://links.lww.com/PAS/B177). Clinical parameters (reduced DLCO and air trapping on CT scans) and reported exposures (SO_2 or burn pits) were equally represented within the subclusters of affected soldiers (Fig. 4A). Consistent with these findings, we did not identify any correlations between clinically detected abnormalities

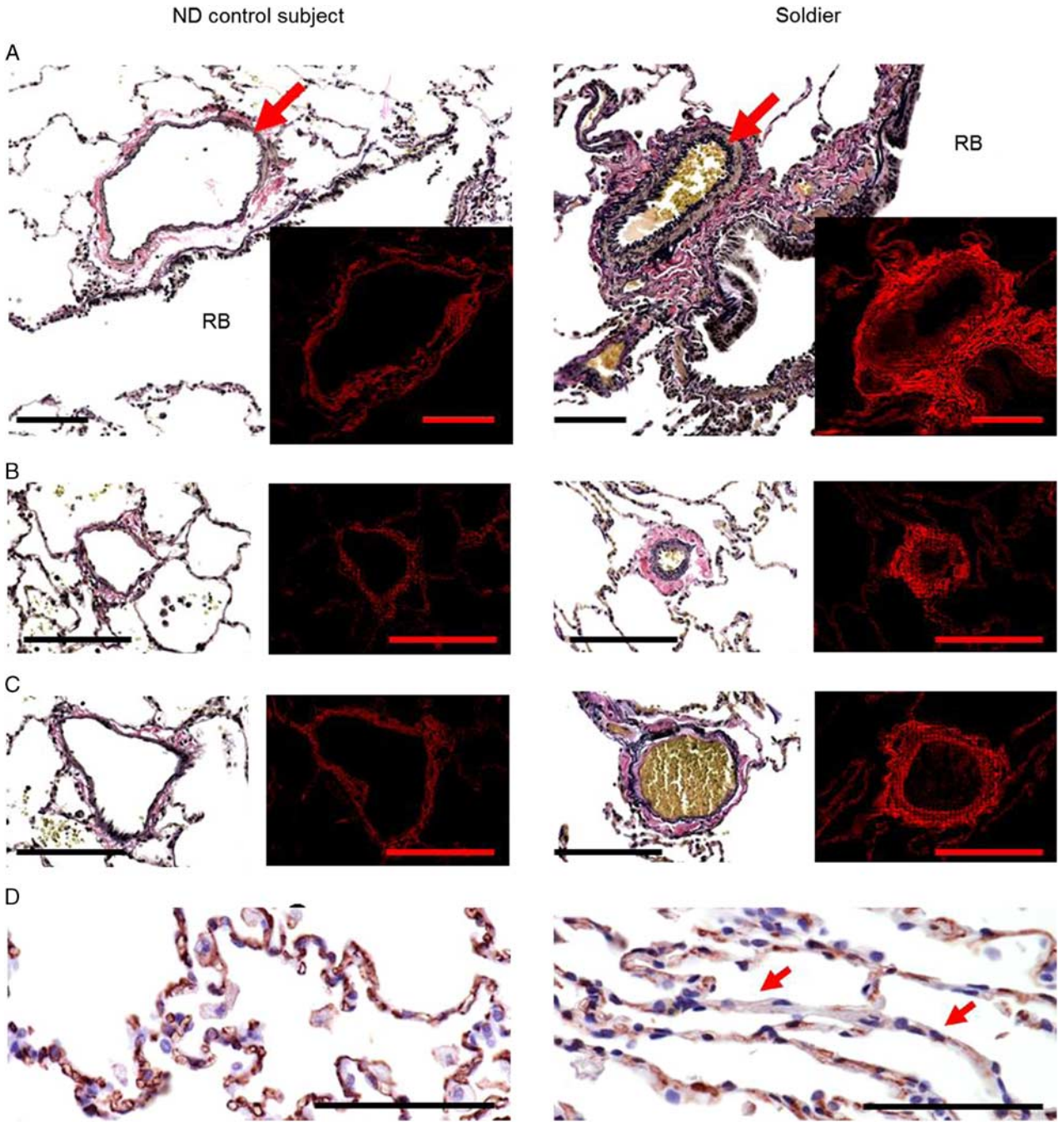

FIGURE 2. Histopathology of distal vasculature. A, Muscularization and fibrosis of distal nonmuscular pulmonary artery (red arrows) adjacent to respiratory bronchioles (RB) in soldier compared with ND control subject. B and C, Increased wall thickness in postcapillary venule (B) and distal venule (C) due to excessive collagen deposition in adventitia in soldier compared with ND control subject. Distal blood vessels located within alveolar tissue and characterized by absence or indistinct internal elastic lamina were considered as pulmonary venules. Venules were considered as postcapillary venules if their size were less than surrounding alveoli or as distal venules if their size were more than surrounding alveoli. A–C, Left images represent Verhoeff-Van Gieson staining; right inserts/images demonstrate collagen red fluorescence on PicroSirius red staining. D, Blood capillaries in IAS in ND control subject and loss of blood capillaries in some IAS (red arrows) in soldier. CD31 immunostaining. Scale bars = 50 μm.

(reduced DLCO or air trapping) or environmental exposures (tobacco smoke, SO_2, or burn pits) and individual pathologic features identified in the lungs of affected soldiers (Supplemental Tables 3 to 7, Supplemental Digital Contents 9 to 13, http://links.lww.com/PAS/B178, http://links.lww.com/PAS/B179, http://links.lww.com/PAS/B180, http://links.lww.com/PAS/B181, http://links.lww.com/PAS/B182).

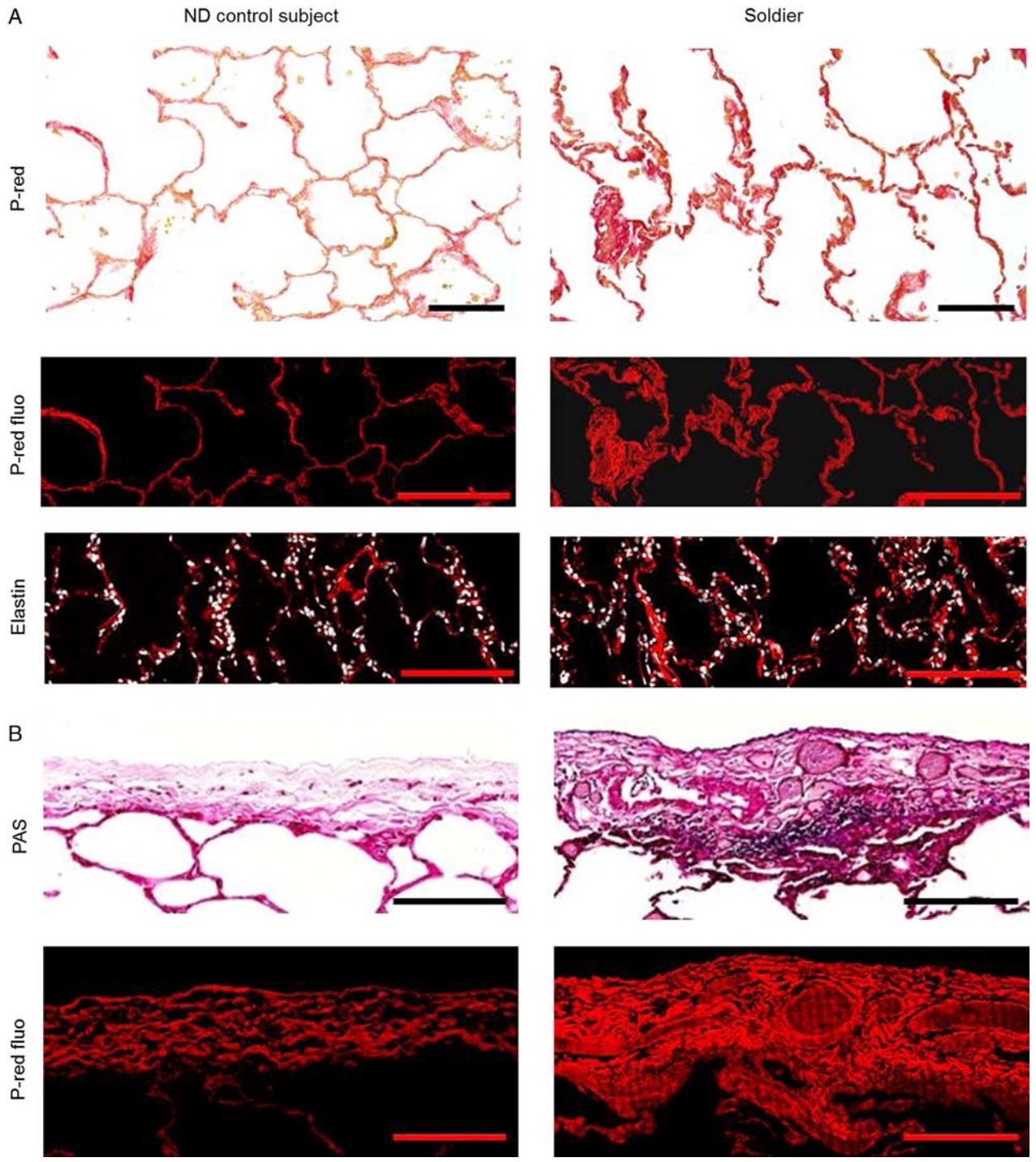

FIGURE 3. Histopathology of alveolar tissue and visceral pleura. A, Top row images illustrate alveolar tissue of ND control subject and soldier (PicroSirius red staining, marked as P-red); middle row—collagen deposition in the IAS of soldier compared with ND control subject (red fluorescence after PicroSirius red staining, marked as P-red fluo); bottom row—elastin deposition in the IAS of soldier compared with ND control subject (red immunofluorescence). B, Top row images illustrate thickening and inflammation of visceral pleura of soldier compared with ND control subject (periodic acid-Schiff [PAS] staining); bottom row—collagen deposition in the pleura of soldier compared with ND control subject (red fluorescence after PicroSirius red staining, marked as P-red fluo). Scale bars = 50 μm.

Using least absolute selection and shrinkage logistic regression analysis, we identified parameters with the most discriminatory power for separating symptomatic soldiers from ND controls. These included: (1) CD4 and CD8 T cell infiltration of small airway walls, (2) medial thickness in distal pulmonary arteries, (3) reduced density of blood capillaries in

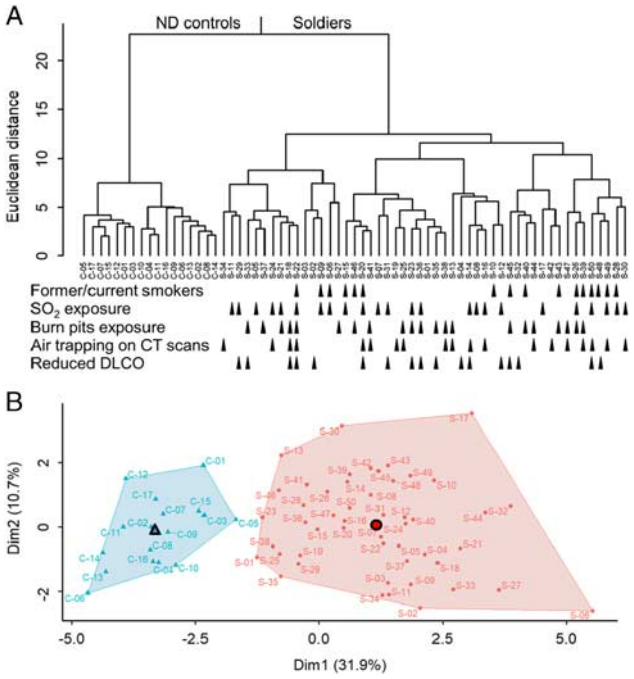

FIGURE 4. Unsupervised hierarchical clustering analysis shows separation of affected soldiers and ND control subjects. A, Unsupervised Hierarchical Clustering Dendrogram using Euclidean distance metric for clustering and calculating the similarity between 2 clusters with Ward method.[18] B, 2-dimension plot where points represent individual subjects according to the 2 principal components that explain the majority of the variance. Dim indicates dimension in 1 direction. Triangle and circle identify the center of each cluster.

IAS, and (4) pleura pathology. Cumulatively, these parameters were sufficient to completely separate the 2 clusters, suggesting that persistent immune cell infiltration, along with pathologic changes in blood vessels and pleura, are conserved aspects of lung pathology in affected soldiers.

DISCUSSION

This study represents a comprehensive case-controlled evaluation of lung pathology in US soldiers with exertional dyspnea and reduced exercise tolerance that persist postdeployment. Histologic and morphometrical evaluation of lung tissue samples from symptomatic soldiers revealed complex pathology characterized by diffuse lymphocytic inflammation, fibrosis of small airways, lung parenchyma and pleura, and hypertensive-type vascular remodeling. On the basis of our findings, it is clear that the previous report that focused on pathologic changes in bronchioles[7] underestimated the nature and extent of lung pathologic remodeling in this cohort of affected soldiers. Therefore, we propose postdeployment respiratory syndrome (PDRS) as a better descriptor for the combination of: (1) history of deployment in Southwest Asia and Afghanistan, (2) inhalational exposures during deployment, (3) chronic respiratory symptoms (reduced exercise tolerance and exertional dyspnea) that develop and persist in the postdeployment period, and (4) lung pathology that affects all distal lung compartments. Together, our quantitative pathologic analysis suggests that diffuse, multicompartment lung pathology contributes to the debilitating respiratory symptoms in these individuals.

Our study confirmed that constrictive bronchiolitis is a component of the lung pathology in affected soldiers. In contrast to classic constrictive bronchiolitis, which can result from exposure to toxic gases or occur secondary to autoimmune disorders,[22–25] constrictive bronchiolitis in soldiers was relatively mild in most cases and not accompanied by fixed airways obstruction and/or air-trapping on chest CT. In the last 2 decades, similar findings of normal spirometry and chest CT scans have been described in biopsy-confirmed case series of constrictive bronchiolitis from Iranian survivors of sulfur mustard gas exposure and studies of flavoring/popcorn factory workers.[26–29] In Gulf War soldiers, it has been difficult to reconcile the degree of dyspnea and exercise intolerance with the diagnosis of constrictive bronchiolitis alone, particularly given the relatively minor PFT abnormalities. However, the widespread nature of lung pathology documented in our study may offer a better explanation of the functional limitations in affected soldiers. Consistent with our findings, lung biopsies from 12 individuals who developed chronic respiratory symptoms after exposure to Word Trade Center dust and fumes after 9/11 showed broad lung pathology with diffuse low-grade lymphocytic inflammation, small airway fibrous remodeling, and areas of interstitial fibrosis and emphysema.[30] The similarities between this report and the pathology seen in affected soldiers with PDRS suggest that large, subacute environmental exposures can induce a syndrome involving pathologic remodeling of multiple compartments in the distal lungs.

Diffuse fibrosis with excessive collagen accumulation in airway walls, blood vessel walls, alveolar tissue, and visceral pleura is a prominent pathologic feature detected in the lungs of soldiers with PDRS. Despite evidence of diffuse fibrotic remodeling, we did not find pathology consistent with identifiable forms of interstitial lung disease, such as usual interstitial pneumonia, nonspecific interstitial pneumonia, or hypersensitivity pneumonitis. While we did not identify substantial distortion of lung parenchyma, honeycombing, or formation of fibroblast foci, we speculate that diffuse interstitial fibrosis, which replaces normal connective tissue with dense collagen deposits, may affect functional lung compliance and contribute to dyspnea on exertion.

In addition to fibrotic remodeling, we identified pathologic changes in pulmonary arteries similar to those described in patients with group 3 pulmonary hypertension.[31–33] Vascular pathology was also present in distal lung vasculature with muscularization of distal pulmonary arteries and reduced capillary density within the IAS. Although the extent of pulmonary vascular remodeling does not appear to be sufficient to cause pulmonary hypertension or RV remodeling detectable by echocardiogram, we suspect that pathologic changes in pulmonary vasculature, along with diffuse fibrotic

remodeling, may explain the reduced exercise tolerance and exertional dyspnea in these soldiers.

Our study has several limitations, including the retrospective nature of data collection and the fact that lungs were not inflated or perfused before fixation. While evaluation of clinical biopsies can lead to some "fixation artifacts," our use of quantitative morphometric techniques with normalization to BM length and comparison to a control group mitigates this concern to some extent. In addition, because the biopsy samples were relatively small in size it is not possible to determine how widespread the pathologic changes are in any individual lung or whether there are regional differences in the lungs of affected soldiers. Our cluster analysis clearly distinguished affected subjects from controls. While this suggests the clinical syndrome is relatively homogenous, the sample size may limit the ability to discern clusters.

In a subset of soldiers with follow-up clinical data, all had continued respiratory symptoms, thus indicating the persistent and unremitting nature of this syndrome. However, our clinical follow-up data must be interpreted with caution since these evaluations are incomplete and not standardized (58% have follow-up clinical evaluation ranging from 1 to 15 y after diagnosis). Despite these limitations, it is striking that none of these patients with longitudinal data available experienced improvement in respiratory symptoms and TLC declined in many soldiers who had follow-up PFTs.

Soldiers with PDRS reported a variety of environmental exposures, including 23 soldiers with self-reported exposure to sulfur dioxide and 21 soldiers exposed to burn pits. While the reported environmental exposures were varied, these soldiers shared common clinical features (cough, dyspnea on exertion, reduced exercise tolerance) and a similar spectrum of lung pathology. Therefore, our study suggests that a variety of different individual exposures (or cumulative exposure to a variety of environmental insults) promote a similar complex of clinical symptoms and pathologic changes in the lungs. Persistent infiltration of airway walls, surrounding alveolar tissue and pleura by T lymphocytes and formation of B cell-containing lymphoid follicles indicate that chronic immune activation is a central feature of this disorder and raises the possibility that the disease could progress over time. Although this idea is supported by the limited follow-up data presented here, additional studies are necessary to confirm whether the disease progresses in affected soldiers and to better identify the environmental exposures that result in PDRS.

REFERENCES

1. Garshick E, Abraham JH, Baird CP, et al. Respiratory Health after Military Service in Southwest Asia and Afghanistan. An Official American Thoracic Society Workshop Report. *Ann Am Thorac Soc*. 2019;16:e1–e16.
2. Krefft SD, Wolff J, Zell-Baran L, et al. Respiratory Diseases in Post-9/11 Military Personnel Following Southwest Asia Deployment. *J Occup Environ Med*. 2020;62:337–343.
3. Sanders JW, Putnam SD, Frankart C, et al. Impact of illness and non-combat injury during Operations Iraqi Freedom and Enduring Freedom (Afghanistan). *Am J Trop Med Hyg*. 2005;73:713–719.
4. Falvo MJ, Osinubi OY, Sotolongo AM, et al. Airborne hazards exposure and respiratory health of Iraq and Afghanistan veterans. *Epidemiol Rev*. 2015;37:116–130.
5. McAndrew LM, Teichman RF, Osinubi OY, et al. Environmental exposure and health of Operation Enduring Freedom/Operation Iraqi Freedom veterans. *J Occup Environ Med*. 2012;54:665–669.
6. Morris MJ, Walter RJ, McCann ET, et al. Clinical Evaluation of Deployed Military Personnel With Chronic Respiratory Symptoms: Study of Active Duty Military for Pulmonary Disease Related to Environmental Deployment Exposures (STAMPEDE) III. *Chest*. 2020;157:1559–1567.
7. King MS, Eisenberg R, Newman JH, et al. Constrictive bronchiolitis in soldiers returning from Iraq and Afghanistan. *N Engl J Med*. 2011; 365:222–230.
8. Szema AM, Schmidt MP, Lanzirotti A, et al. Titanium and iron in lung of a soldier with nonspecific interstitial pneumonitis and bronchiolitis after returning from Iraq. *J Occup Environ Med*. 2012; 54:1–2.
9. Lentz RJ, Fessel JP, Johnson JE, et al. Transbronchial cryobiopsy can diagnose constrictive bronchiolitis in veterans of recent conflicts in the Middle East. *Am J Respir Crit Care Med*. 2016;193:806–808.
10. Weiler BA, Colby TV, Floreth TJ, et al. Small airways disease in an Operation Desert Storm Deployer: case report and review of the literature on respiratory health and inhalational exposures from Gulf War I. *Am J Ind Med*. 2018;61:793–801.
11. Morris MJ, Lucero PF, Zanders TB, et al. Diagnosis and management of chronic lung disease in deployed military personnel. *Ther Adv Respir Dis*. 2013;7:235–245.
12. Morris MJ, Rawlins FA, Forbes DA, et al. Deployment-related respiratory issues. *US Army Med Dep J*. 2016;2-16:173–178.
13. Banks DE, Bolduc CA, Ali S, et al. Constrictive bronchiolitis attributable to inhalation of toxic agents: considerations for a case definition. *J Occup Environ Med*. 2018;60:90–96.
14. Culver BH, Graham BL, Coates AL, et al. Recommendations for a standardized pulmonary function report. An Official American Thoracic Society Technical Statement. *Am J Respir Crit Care Med*. 2017;196:1463–1472.
15. Rudski LG, Lai WW, Afilalo J, et al. Guidelines for the echocardiographic assessment of the right heart in adults: a report from the American Society of Echocardiography endorsed by the European Association of Echocardiography, a registered branch of the European Society of Cardiology, and the Canadian Society of Echocardiography. *J Am Soc Echocardiogr*. 2010;23:685–713.
16. Lang RM, Badano LP, Mor-Avi V, et al. Recommendations for cardiac chamber quantification by echocardiography in adults: an update from the American Society of Echocardiography and the European Association of Cardiovascular Imaging. *J Am Soc Echocardiogr*. 2015;28:1–39.
17. Hsia CC, Hyde DM, Ochs M, et al. An official research policy statement of the American Thoracic Society/European Respiratory Society: standards for quantitative assessment of lung structure. *Am J Respir Crit Care Med*. 2010;181:394–418.
18. Murtagh F, Legendre P. Ward's Hierarchical Agglomerative Clustering Method: Which Algorithms Implement Ward's Criterion? *J Classif*. 2014;31:274–295.
19. Tibshirani R, Walther G, Hastie T. Estimating the number of clusters in a data set viathe gap statistic. *J R Statist Soc B*. 2001; 63:411–423.
20. Friedman J, Hastie T, Tibshirani R. Regularization Paths for Generalized Linear Models via Coordinate Descent. *J Stat Softw*. 2010;33:1–22.
21. Carn SA, Krueger AJ, Krotkov NA, et al. Fire at Iraqi sulfur plant emits SO2 clouds detected by Earth Probe TOMS. *Geophys Res Lett*. 2004;31:L19105.
22. Horvath EP, doPico GA, Barbee RA, et al. Nitrogen dioxide-induced pulmonary disease: five new cases and a review of the leterature. *J Occup Med*. 1978;20:103–110.
23. Woodford DM, Coutu RE, Gaensler EA. Obstructive lung disease from acute sulfur dioxide exposure. *Respiration*. 1979;38:238–245.
24. Weiss SM, Lakshminarayan S. Acute inhalation injury. *Clin Chest Med*. 1994;15:103–116.

25. Krefft SD, Cool CD, Rose CS. The emerging spectrum of exposure-related bronchiolitis. *Curr Opin Allergy Clin Immunol*. 2018;18:87–95.
26. Markopoulo KD, Cool CD, Elliot TL, et al. Obliterative bronchiolitis: varying presentations and clinicopathological correlation. *Eur Respir J*. 2002;19:20–30.
27. Ghanei M, Tazelaar HD, Chilosi M, et al. An international collaborative pathologic study of surgical lung biopsies from mustard gas-exposed patients. *Respir Med*. 2008;102:825–830.
28. Figueiredo S, Morais A, Magalhaes A, et al. Occupational constrictive bronchiolitis with normal physical, functional and image findings. *Rev Port Pneumol*. 2009;15:729–732.
29. Ghanei M, Ghayumi M, Ahakzani N, et al. Noninvasive diagnosis of bronchiolitis obliterans due to sulfur mustard exposure: could high-resolution computed tomography give us a clue? *Radiol Med*. 2010;115:413–420.
30. Caplan-Shaw CE, Yee H, Rogers L, et al. Lung pathologic findings in a local residential and working community exposed to World Trade Center dust, gas, and fumes. *J Occup Environ Med*. 2011;53:981–991.
31. Wright JL, Levy RD, Churg A. Pulmonary hypertension in chronic obstructive pulmonary disease: current theories of pathogenesis and their implications for treatment. *Thorax*. 2005;60:605–609.
32. Tuder RM. Pathology of pulmonary arterial hypertension. *Semin Respir Crit Care Med*. 2009;30:376–385.
33. Tuder RM. Pulmonary vascular remodeling in pulmonary hypertension. *Cell Tissue Res*. 2017;367:643–649.